

LA-UR-15-26769  
August 27, 2015



# Corner gradient reconstruction (CGR) and the reduction of dissipation in Lagrange cell-centered hydrodynamics (CCH)

D.E. Burton, N.R. Morgan, T.C. Carney, M.A. Kenamond, B.J. Brown  
X-Computational Physics Division  
Los Alamos National Laboratory

**MultiMat 2015**  
International Conference on Numerical Methods for Multi-Material Fluid Flows  
Wurzburg, September 7-11, 2015



**Acknowledgement:**  
LANL ASC & LDRD programs

# Our principal goals are to reduce dissipation in cell-centered hydro (CCH) and to improve accuracy in ALE schemes

## Motivation:

Cell centered hydro (CCH) schemes produce excellent results on many test problems, but appear too dissipative on others

Similarly, swept face advection is satisfactory for many problems, but it performs poorly on others

## We wish to:

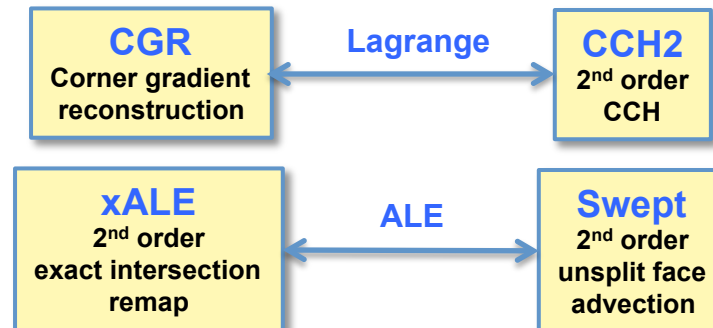
Reduce dissipation in CCH by introducing a new variation called **Corner Gradient Reconstruction (CGR<sup>\*\*</sup>)**

Improve smooth flow solutions without degrading those with shocks

Achieve higher order accuracy within the framework of linear cell faces

Although we focus on our particular implementation (**CCH2<sup>\*</sup>**), the method should be beneficial in other CCH formulations

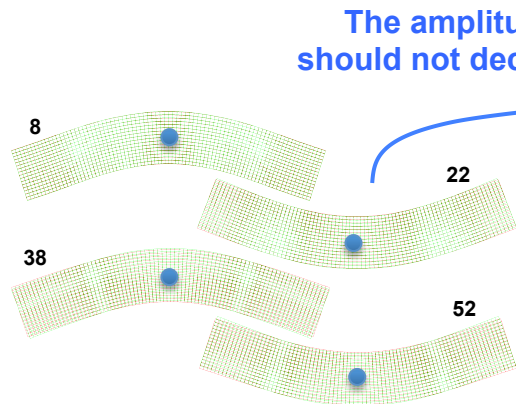
We will contrast **CGR & xALE<sup>\*\*\*</sup>** with previous methods:



\* C&F 2012  
\*\* JCP 2015  
\*\*\* MultiMat 2013

# Motivation: CCH2 dissipates kinetic energy in shockless problems such as an elastic bending plate

Large deformation of an elastic Be Plate  
Initial velocity field activates only first flexural mode  
80x16 cells  
Times are near maxima of displacement

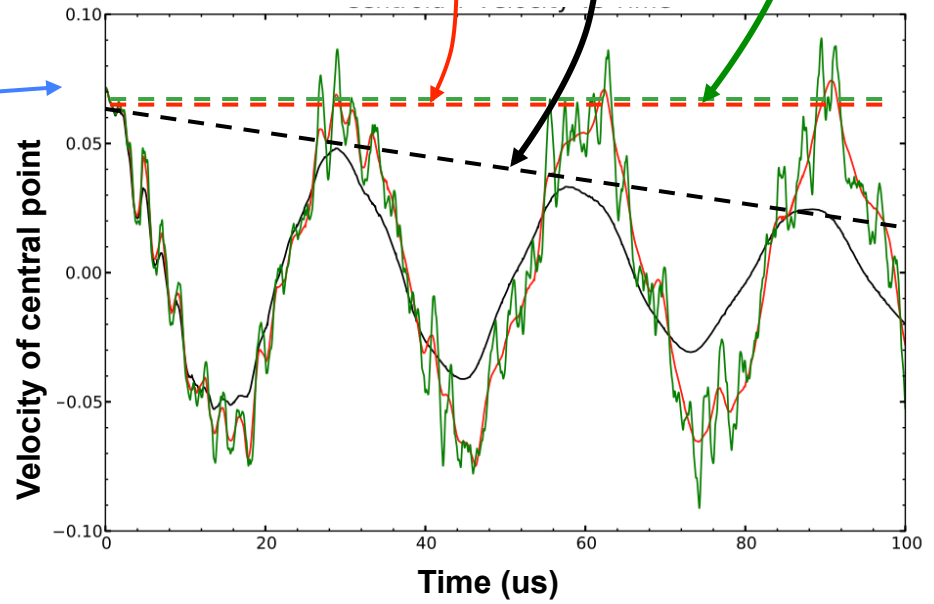


Weseloh, Pagosa  
Sample Problems, 2011

Reference: SGH with Q artificially set to 0 –  
impractical, but possible for smooth flow.  
Noisy, but does not dissipate kinetic energy

CCH2: Loses amplitude and  
is clearly more dissipative

CGR: Free of excess dissipation  
Amplitude essentially constant



# Lagrange CCH overview: There are three steps of interest - Note that “conservation” has 2 different contexts

**Finite volume method:** Cell averages are found by integrating surface fluxes

$$M_z \dot{\mathbf{u}}_z = \oint_z d\mathbf{N} \cdot \boldsymbol{\sigma} \rightarrow \sum_i^z \mathbf{N}^i \cdot \boldsymbol{\sigma}_p^i$$

**The challenge in CCH is the determination of the surface fluxes  $\mathbf{u}_p$  &  $\boldsymbol{\sigma}_p$**

**Conservative reconstruction:** Finite volume provides no information about the distribution of quantities within a cell.

Infer a distribution by fitting to adjacent cells & requiring conservation within the cell

$$V_z \mathbf{u}_z = \oint_z \mathbf{u}(\mathbf{x}) dV$$

$$V_z \boldsymbol{\sigma}_z = \oint_z \boldsymbol{\sigma}(\mathbf{x}) dV$$

This yields discontinuous values of at the cell surface  $\mathbf{u}_c$  &  $\boldsymbol{\sigma}_c$

**CGR differs from traditional CCH2 only in the reconstruction**

**Flux conservation** requires the sum of the fluxes at nodes to vanish

$$\sum_i^p \mathbf{N}^i \cdot \boldsymbol{\sigma}_p^i = 0$$

$$\sum_i^p \mathbf{N}^i \cdot \mathbf{u}_p^i = 0$$

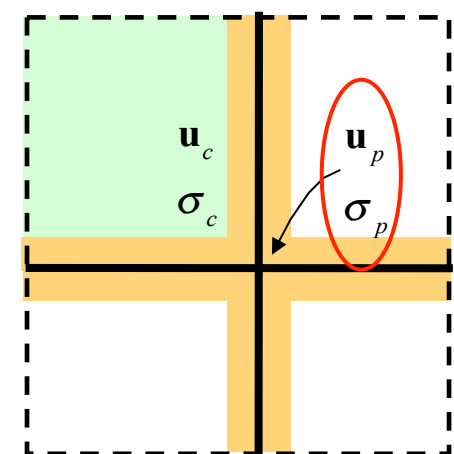
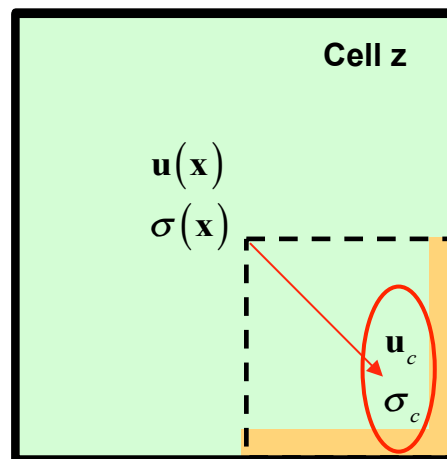
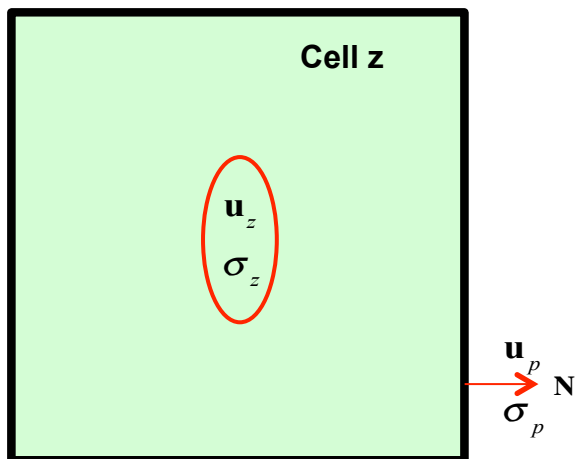
**A dissipation relation enforces the 2<sup>nd</sup> law**

$$\mathbf{N} \cdot (\boldsymbol{\sigma}_p - \boldsymbol{\sigma}_c) \cdot (\mathbf{u}_p - \mathbf{u}_c) \geq 0$$

**An approximate Riemann solution determines the fluxes**

$$\mathbf{u}_p \text{ & } \boldsymbol{\sigma}_p$$

**& completes the cycle**



## Now consider some alternative polynomial reconstructions for the Lagrange phase\*

PPM-like (black) is 3<sup>rd</sup> order and the most accurate

However, 3D requires an expensive solution to a 10 equation system for each of 3 velocity components and 6 stress components

$$\begin{aligned}
 u^k(\mathbf{x}) = & u_o^k \\
 & + a_1^k \delta x + a_2^k \delta y + a_3^k \delta z \\
 & + a_{11}^k \delta x^2 + a_{22}^k \delta y^2 + a_{33}^k \delta z^2 \\
 & + a_{12}^k \delta x \delta y + a_{13}^k \delta x \delta z + a_{23}^k \delta y \delta z
 \end{aligned}$$

CCH2 (blue) uses the traditional 2<sup>nd</sup> order reconstruction

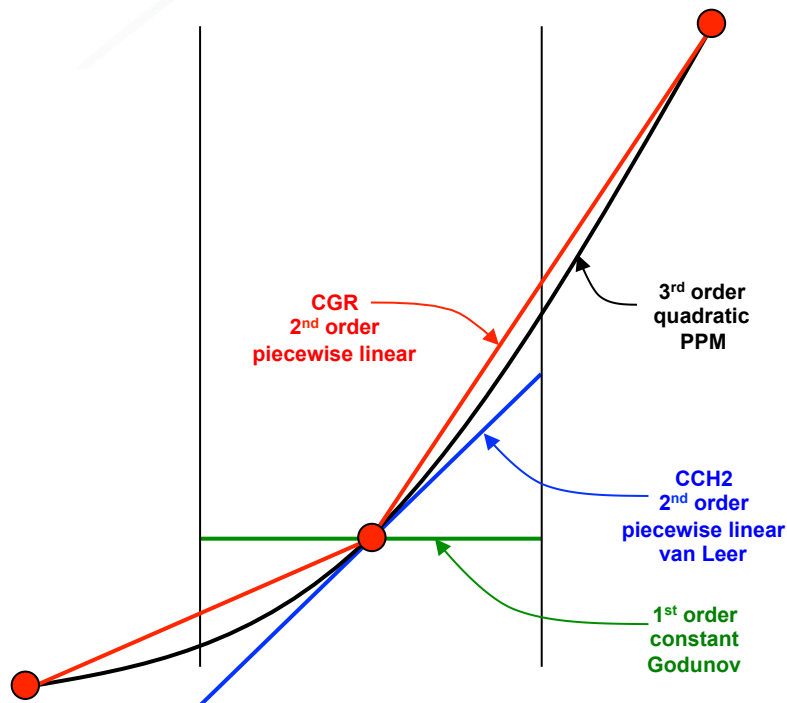
Requires only Cramer's rule.

Corner gradient reconstruction (CGR - red) uses a piecewise linear fit between cell averages

Also requires only Cramer's rule

Although formally 2<sup>nd</sup> order, CGR is a much closer representation of the 3<sup>rd</sup> order function

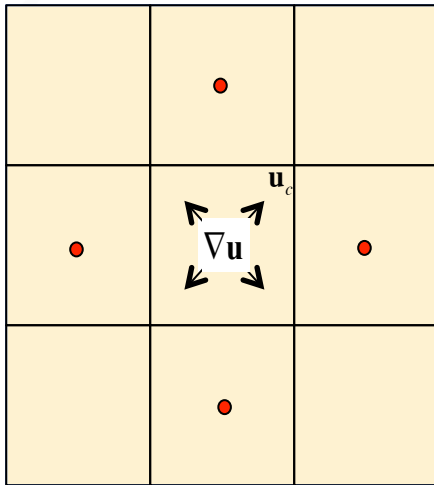
CGR captures a 3<sup>rd</sup> order characteristic: differing slopes within a cell



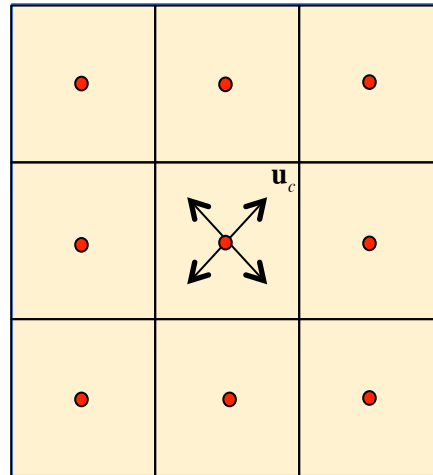
\* The notion of "reconstruction" is common in Eulerian advection, but seldom thought about in the Lagrange step

# For regular grids in 2D, the stencils for the reconstruction polynomials reduce to:

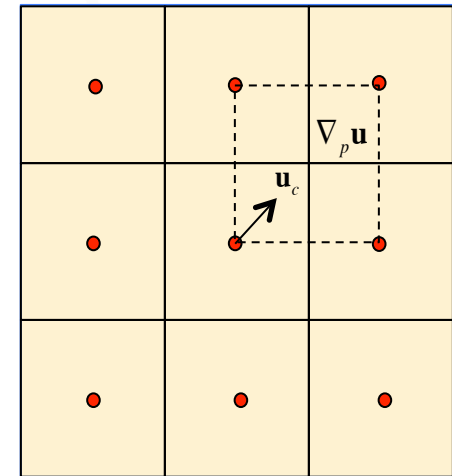
CCH2 uses a 4 point stencil and is **inaccurate at the corners**



3<sup>rd</sup> order uses a 9-point stencil is **more accurate at the corners than 2<sup>nd</sup> order**



CGR stencil is effectively 9-point and is **more accurate at the corners than 2<sup>nd</sup> order**



9-point stencils require special handling of ghost cells at mesh corners

# When should dissipation occur? Smooth flows should not dissipate

Our goal is the reduction of dissipation, not necessarily the most accurate polynomial reconstruction

We need a numerical notion of “smooth flow”

Consider velocity

Fit a polynomial across a cell and its neighbors (**red**) such that the integral is conserved:

$$V_z \mathbf{u}_z = \oint_z \mathbf{u}(\mathbf{x}) dV$$

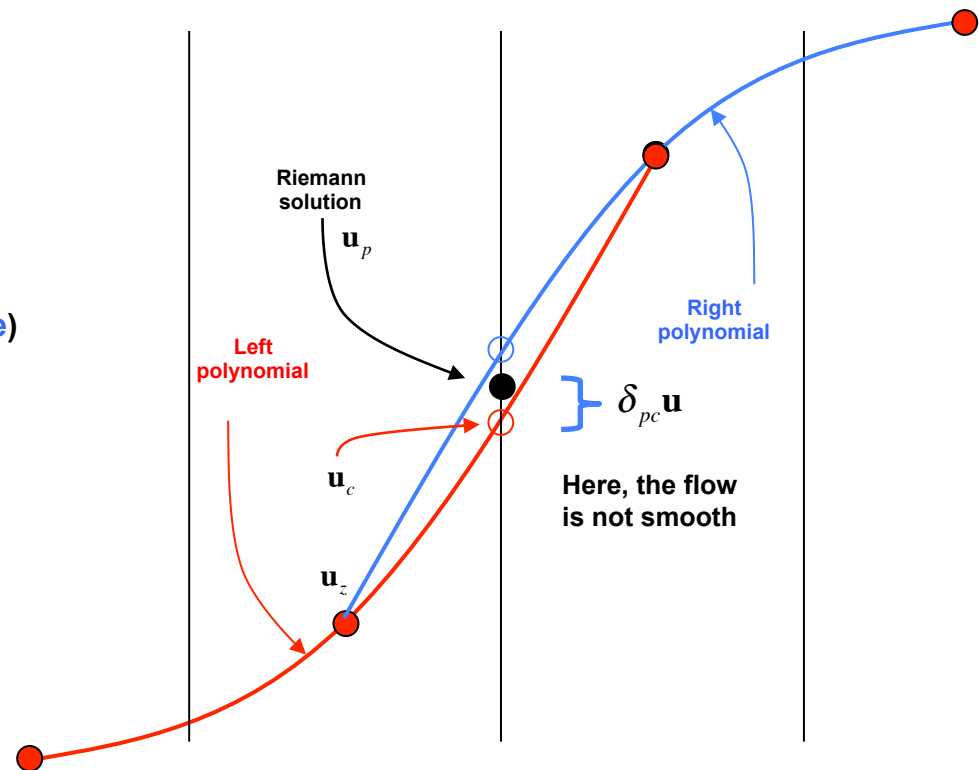
Then do the same for an adjacent cell (**blue**)

If the polynomials are coincident at the interface,  
the flow is locally smooth

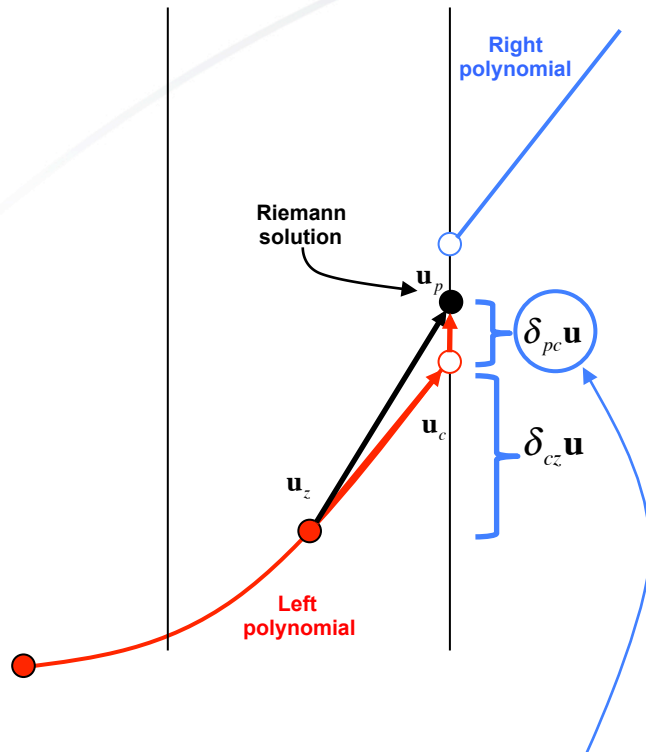
and there should be no dissipation

If not, the discontinuity  
is the source of dissipation

and is resolved by an approximate  
Riemann solution that yields  $\delta_{pc} \mathbf{u}$



# How does the discontinuity affect the total energy and the decomposition into kinetic and internal energy?



The surface fluxes can be decomposed into a **reconstruction** and a **discontinuity**

$$\mathbf{u}_p = \mathbf{u}_z + \delta_{cz} \mathbf{u} + \delta_{pc} \mathbf{u}$$

$$\boldsymbol{\sigma}_p = \boldsymbol{\sigma}_z + \delta_{cz} \boldsymbol{\sigma} + \delta_{pc} \boldsymbol{\sigma}$$

With this substitution,

the total energy rate equation can then be exactly decomposed into a sum of **kinetic**  $\dot{K}_z$  & **internal**  $\dot{E}_z$  contributions

$$\begin{aligned} \dot{T}_z &= \oint_z d\mathbf{N} \cdot (\boldsymbol{\sigma}_p \cdot \mathbf{u}_p) \\ &= \dot{K}_z + [\dot{W}_z + \dot{R}_z + \dot{D}_z] \end{aligned}$$

in which

<b>Kinetic energy</b>	$\dot{K}_z = \left[ \oint_z d\mathbf{N} \cdot \boldsymbol{\sigma}_p \right] \cdot \mathbf{u}_z = \dot{\mathbf{U}}_z \cdot \mathbf{u}_z$
<b>Reversible work due to average stress</b>	$\dot{W}_z = \boldsymbol{\sigma}_z : \left[ \oint_z d\mathbf{N} \mathbf{u}_p \right] = \boldsymbol{\sigma}_z : \dot{\boldsymbol{\Gamma}}_z$
<b>Work due to the reconstruction</b>	$\dot{R}_z = \oint_z d\mathbf{N} \cdot (\delta_{cz} \boldsymbol{\sigma} \cdot \delta_{pc} \mathbf{u} + \delta_{cz} \mathbf{u} \cdot \delta_{pc} \boldsymbol{\sigma})$
<b>Irreversible dissipation</b>	$\dot{D}_z = \oint_z d\mathbf{N} \cdot \mu \dot{\mathbf{n}} (\delta_{pc} \mathbf{u})^2 \geq 0$

The source of dissipation lies in the  $\dot{D}_z$  &  $\dot{R}_z$  terms

Reconstruction reduces the dissipation by reducing the discontinuity  $\delta_{pc} \mathbf{u}$

# In CGR, discontinuity & dissipation occur only when “curvature” requires a shift to guarantee conservative reconstruction

In each cell corner

$$\mathbf{u}(\mathbf{x}) = \mathbf{u}_0 + \beta(\mathbf{x} - \mathbf{x}_z) \cdot \nabla_p \mathbf{u}$$

The left and right polynomials are initially coincident (black), corresponding to no dissipation

However, a change in slope within the cell (“curvature”) requires a shift to guarantee conservation

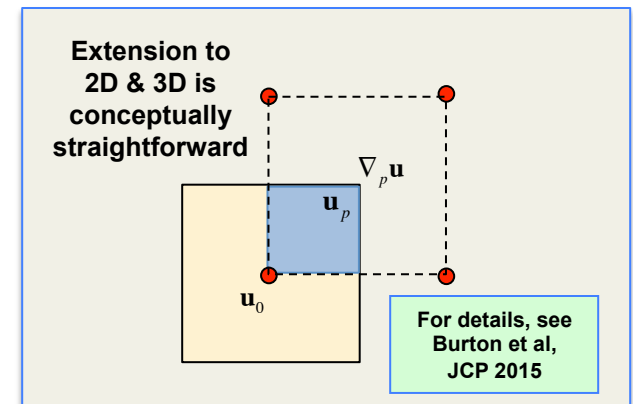
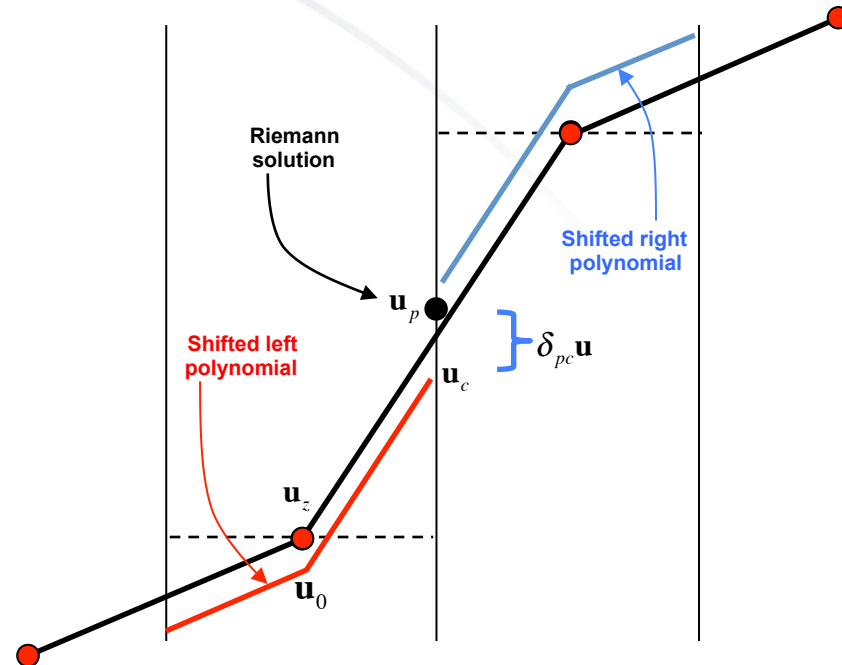
$$V_z \mathbf{u}_z = \oint_z \mathbf{u}(\mathbf{x}) dV$$

This results in a discontinuity at the interface and therefore dissipation

No shift occurs when the slopes within the cell are identical

Monotonicity is enforced by limiting the gradient with a Barth-Jespersen scheme.

Because the slope affects the conservation integral, the limiter  $\beta$  and the shift  $\mathbf{u}_0(\beta)$  are coupled



# We tested CGR (& xALE) under a wide variety of conditions

## Hydro:

Lagrange  
Swept face advection  
Exact intersection remap

## Geometry:

1D (X)  
2D (XY RZ)  
3D (XYZ)

## Flow:

Smooth  
Vortical  
Shock

## Meshes:

Rectangular  
Polar  
Skewed

## Materials:

Fluids  
Elastic  
Elastic-plastic solids  
Elastic-plastic hardening

Problem	Dim	Geom	Mesh	Hydro	Material	Flow	
Be plate	2D	XY	Square	Lag	Elastic	Smooth	
Taylor-Green	2D	XY	Square	Lag	Gas	Smooth+vorticity	
Coggeshall	2D	XY	Square	Lag	Gas	Smooth	
	3D	XYZ	Square	Lag	Gas	Smooth	
Kidder shell	2D	RZ	Polar	Lag	Gas	Smooth	
	3D	XYZ	Special	Lag	Gas	Smooth	
Kidder ball	2D	RZ	Square	Lag	Gas	Smooth	
Howell	2D	XY	Polar	Lag	EP	Smooth	
Verney	2D	RZ	Polar	Lag	EP	Smooth	
	3D	XYZ	Geo	Lag	EP	Smooth	
Taylor Anvil	2D	RZ	Square	Lag	EP+hardening	Shock+smooth	
Sod	2D	XY	Rect	Lag	Gas	Shock	
	Noh	2D	XY	Polar	Lag	Gas	Shock
		2D	RZ	Polar	Lag	Gas	Shock
	2D	XY	Square	Lag	Gas	Shock	
	2D	RZ	Square	Lag	Gas	Shock	
	3D	XYZ	Square	Lag	Gas	Shock	
Sedov	2D	XY	Square	Lag	Gas	Shock	
	2D	RZ	Square	Lag	Gas	Shock	
	3D	XYZ	Square	Lag	Gas	Shock	
Saltzman	2D	XY	Special	Lag	Gas	Shock	
	2D	RZ	Special	Lag	Gas	Shock	
	3D	XYZ	Special	Lag	Gas	Shock	
Adiabatic rel	1D	X	Rect	Lag	Gas	Shock+release	
EP piston	1D	X	Rect	Lag	EP	Shock	
Triple point	2D	XY	Square	ALE	Gas	Shock+vorticity	
He bubble	2D	RZ	Rect	ALE	Gas	Shock+vorticity	



# SMOOTH & VORTICAL FLOW PROBLEMS

**Be Beam (elastic solid)**

**Taylor-Green (vortical flow)**

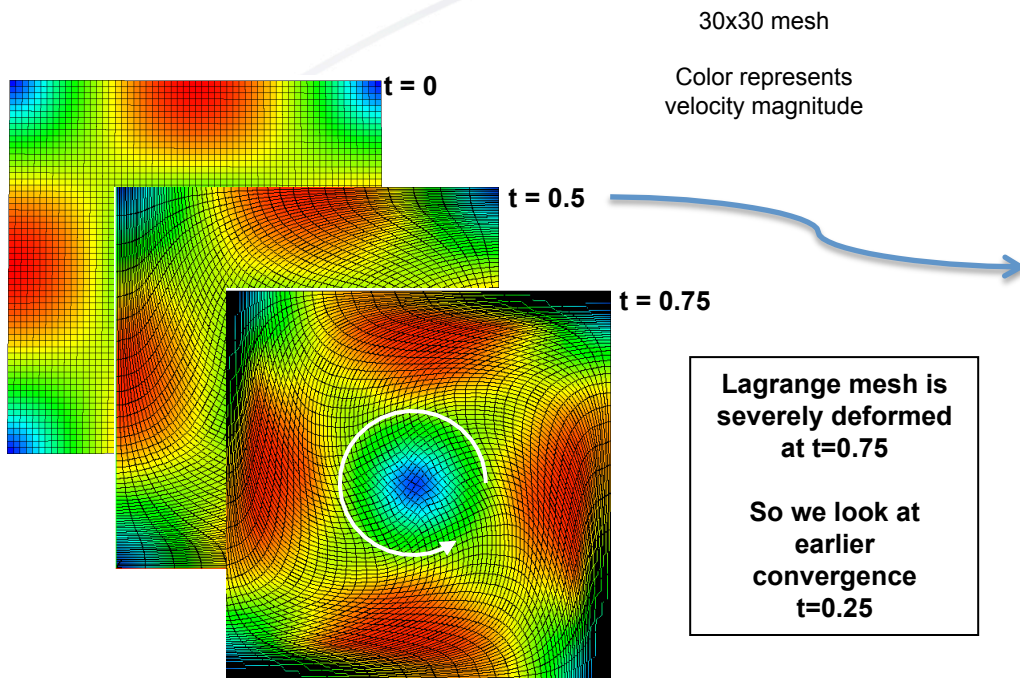
**Coggeshall**

**Kidder shell & ball**

**Verney & Howell (elastic-plastic solid)**

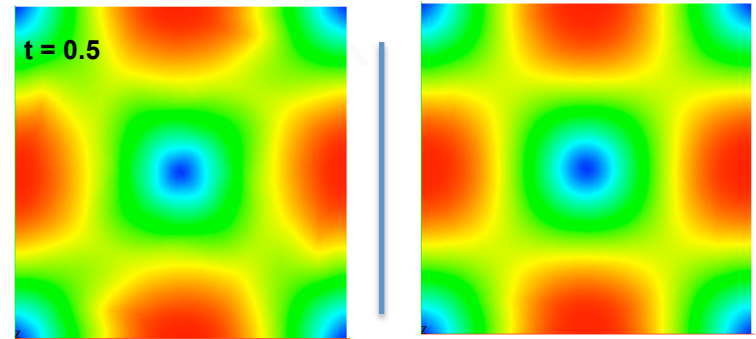
**Taylor anvil (hardening EP solid)**

# 2D Taylor Green is a test of vortical flow: CGR reduces the error & has a convergence rate approaching 3<sup>rd</sup> order



Lagrange mesh is severely deformed at t=0.75  
So we look at earlier convergence t=0.25

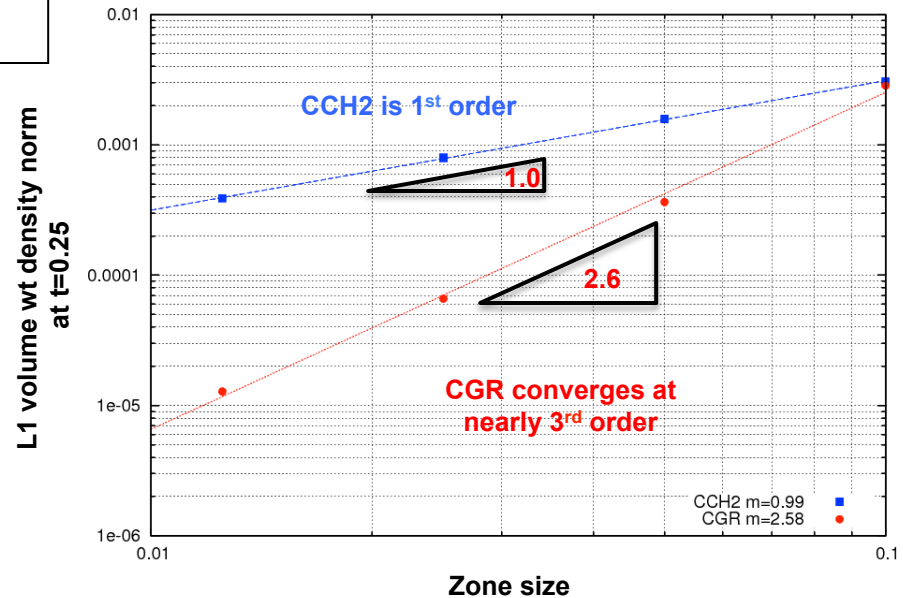
Velocity contours should remain stationary in time  
CCH2  
CGR is significantly better



The flow should be incompressible and the velocity field should not change with time

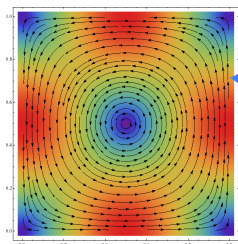
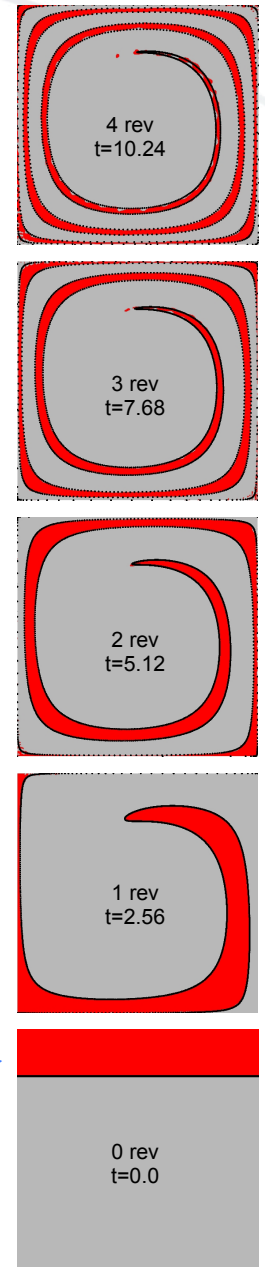
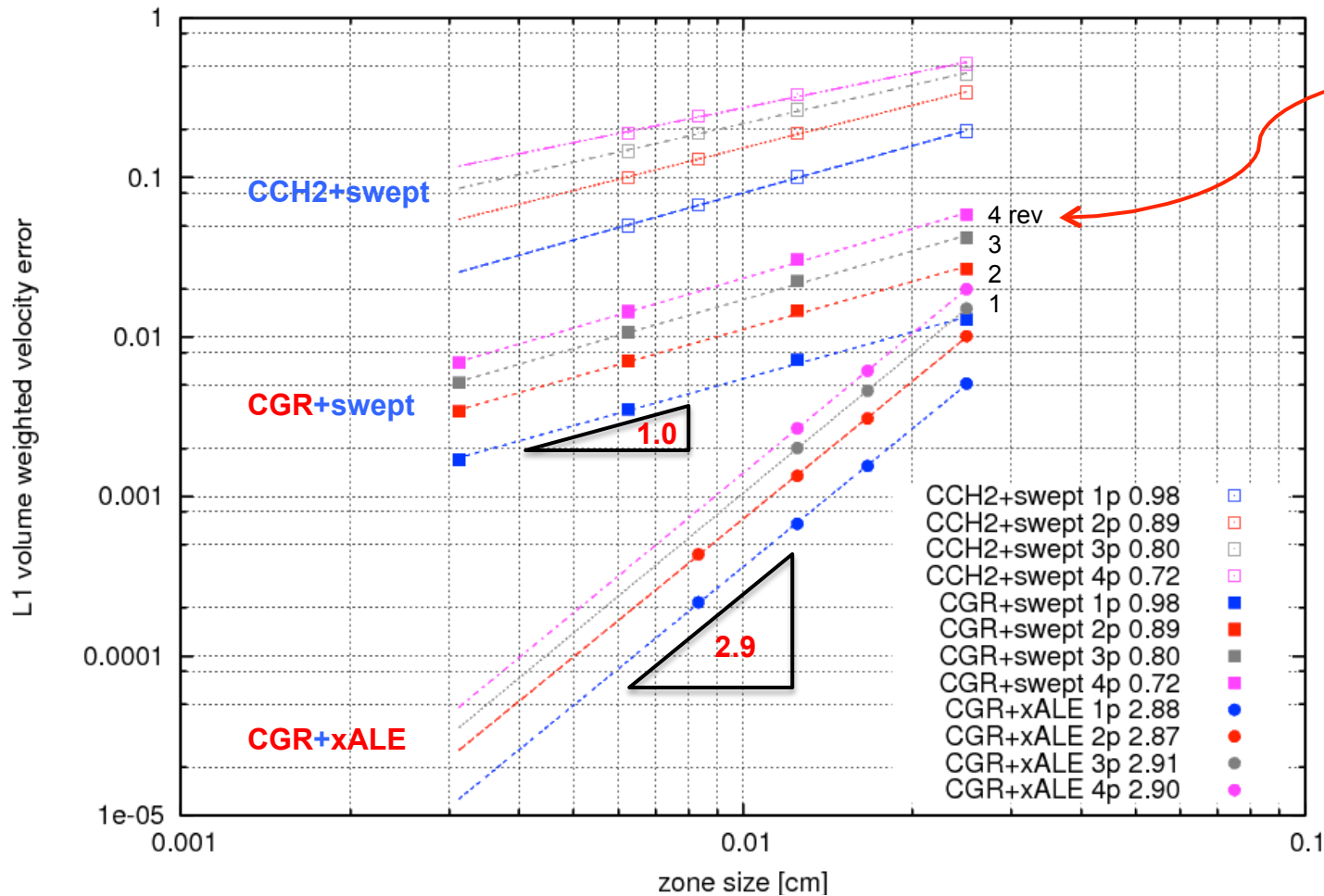
$$\mathbf{u}_0 = \{ \sin(\pi x) \cos(\pi y), -\cos(\pi x) \sin(\pi y) \}$$

The solution also involves a time dependent energy source from a manufactured solution



Taylor & Green, 1937  
Drikakis et al, 2007  
Dobrev et al 2012  
Burton et al 2015

# Using ALE, we can run Taylor-Green through multiple revolutions: CGR + xALE improves accuracy and convergence to near 3<sup>rd</sup> order



Related TG calculation with material interfaces to illustrate rotation.  
Black is the analytic solution

Brown & Morgan 2015

# Spherical Coggeshall problem on a box grid: CCH2 has large perturbations not present in CGR

Shock-free spherical compression of polytropic gas with initial linear velocity field  $u_0(r)=-r_0$

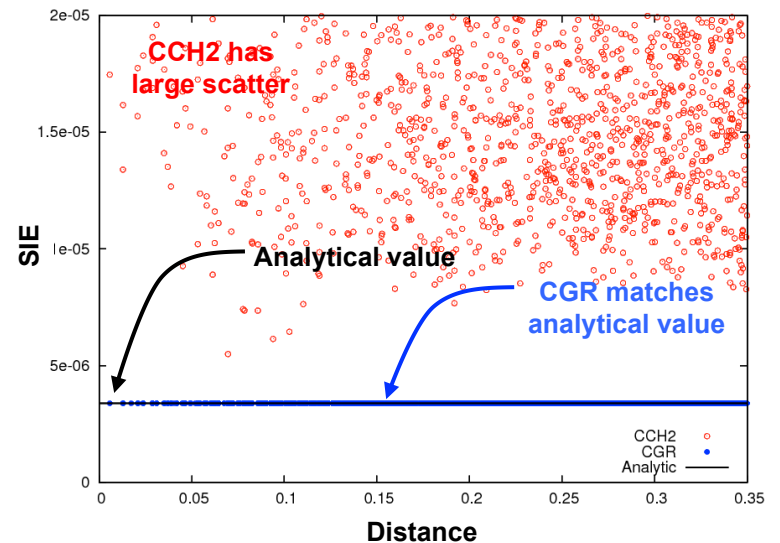
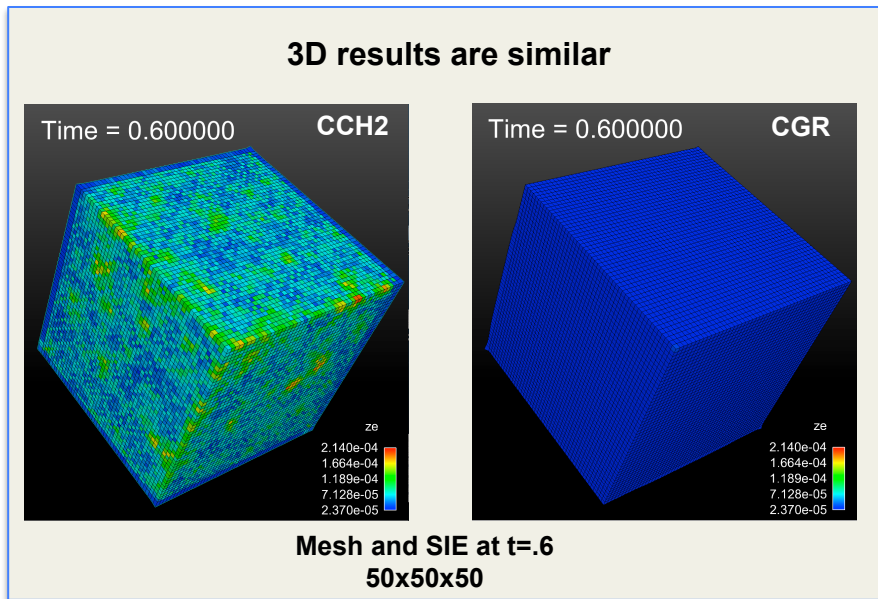
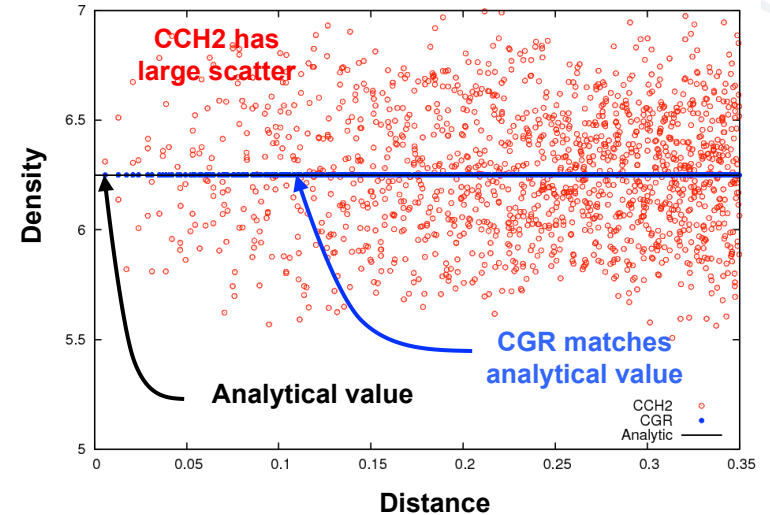
The problem is characterized by high specific kinetic energy ( $\sim 1$ ) and low internal energy ( $\sim 1e-6$ ).

Relatively small velocity perturbations give rise to large error in thermodynamic variables.

Scatter plots:  
one dot per cell

Exact solutions  
in black

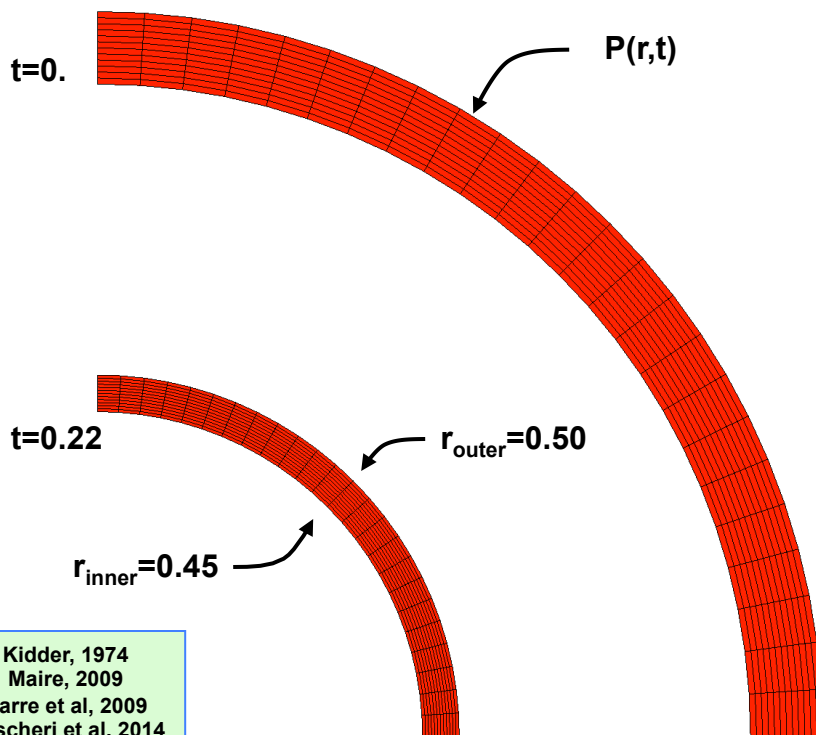
SIE = specific internal energy



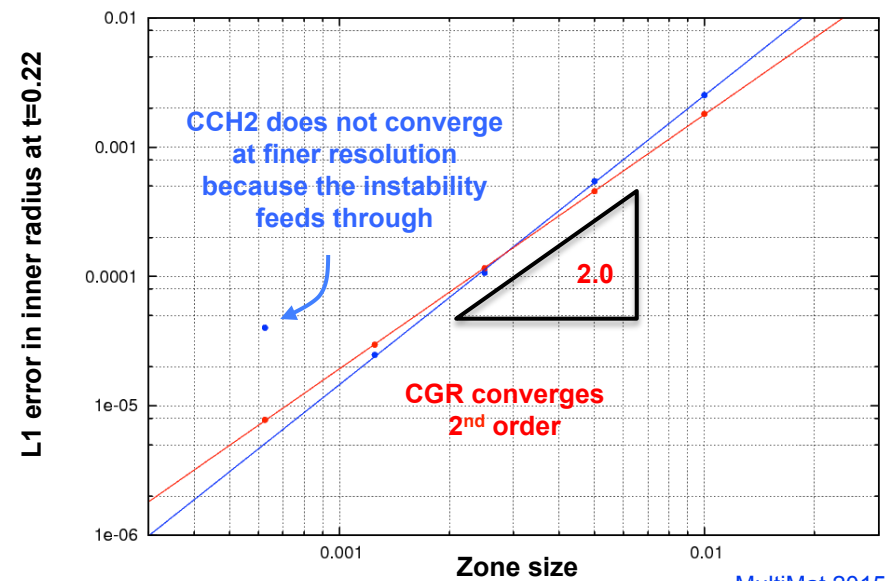
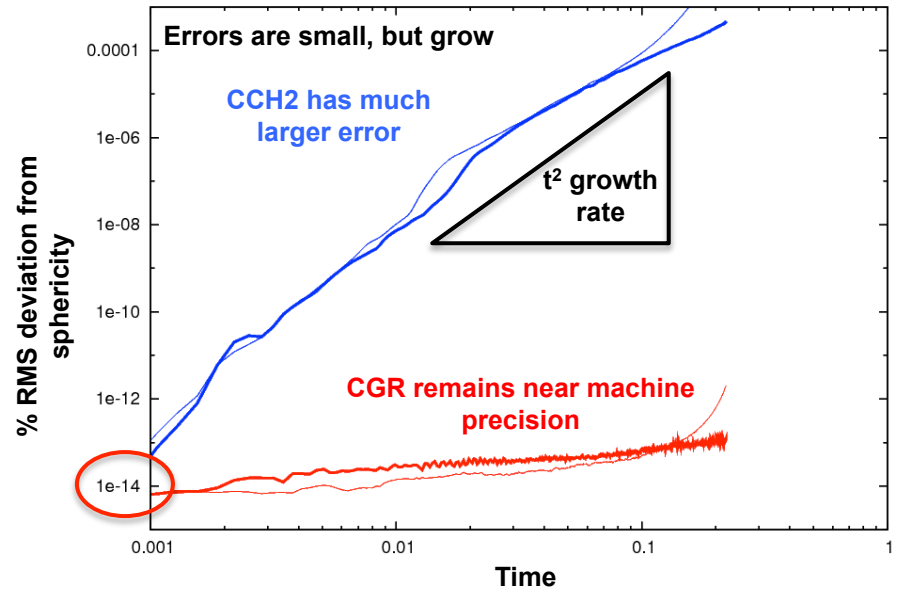
# 2D Kidder shell tests symmetry: Given $P(r,t)$ at outer surface compare with analytic $r(t)$

Because the surface has an Atwood number of unity, it is hydrodynamically unstable, and therefore sensitive to numerical perturbations

In 2D, near perfect grids mitigate the error



Inner (heavy) and outer (light) radii

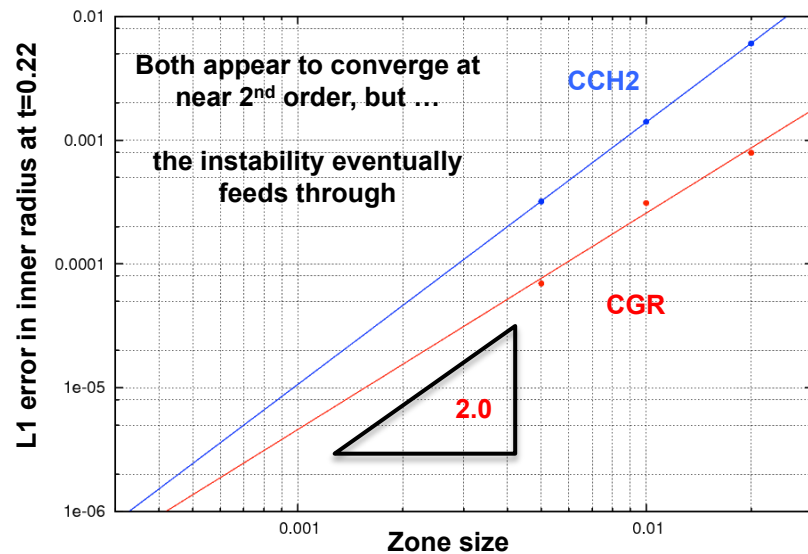
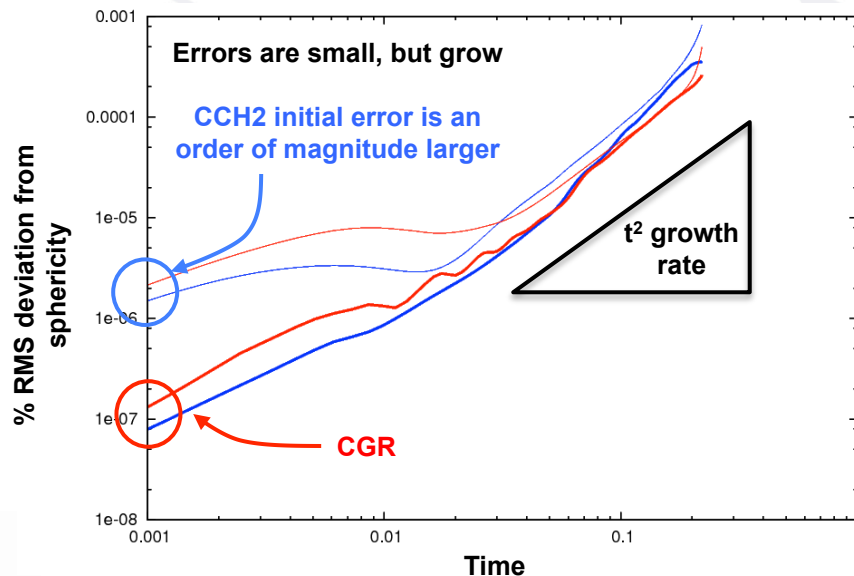
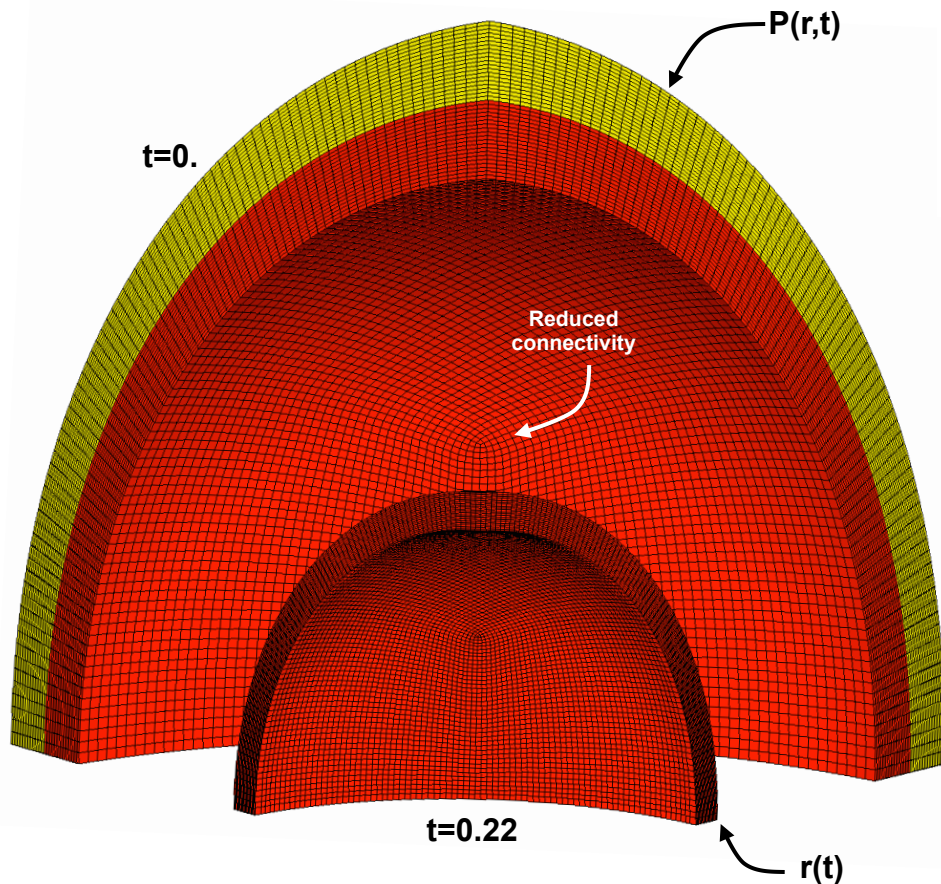


- Kidder, 1974
- Maire, 2009
- Carre et al, 2009
- Boscheri et al, 2014
- Villar et al, 2014
- Morgan et al, 2015
- Burton et al, 2015

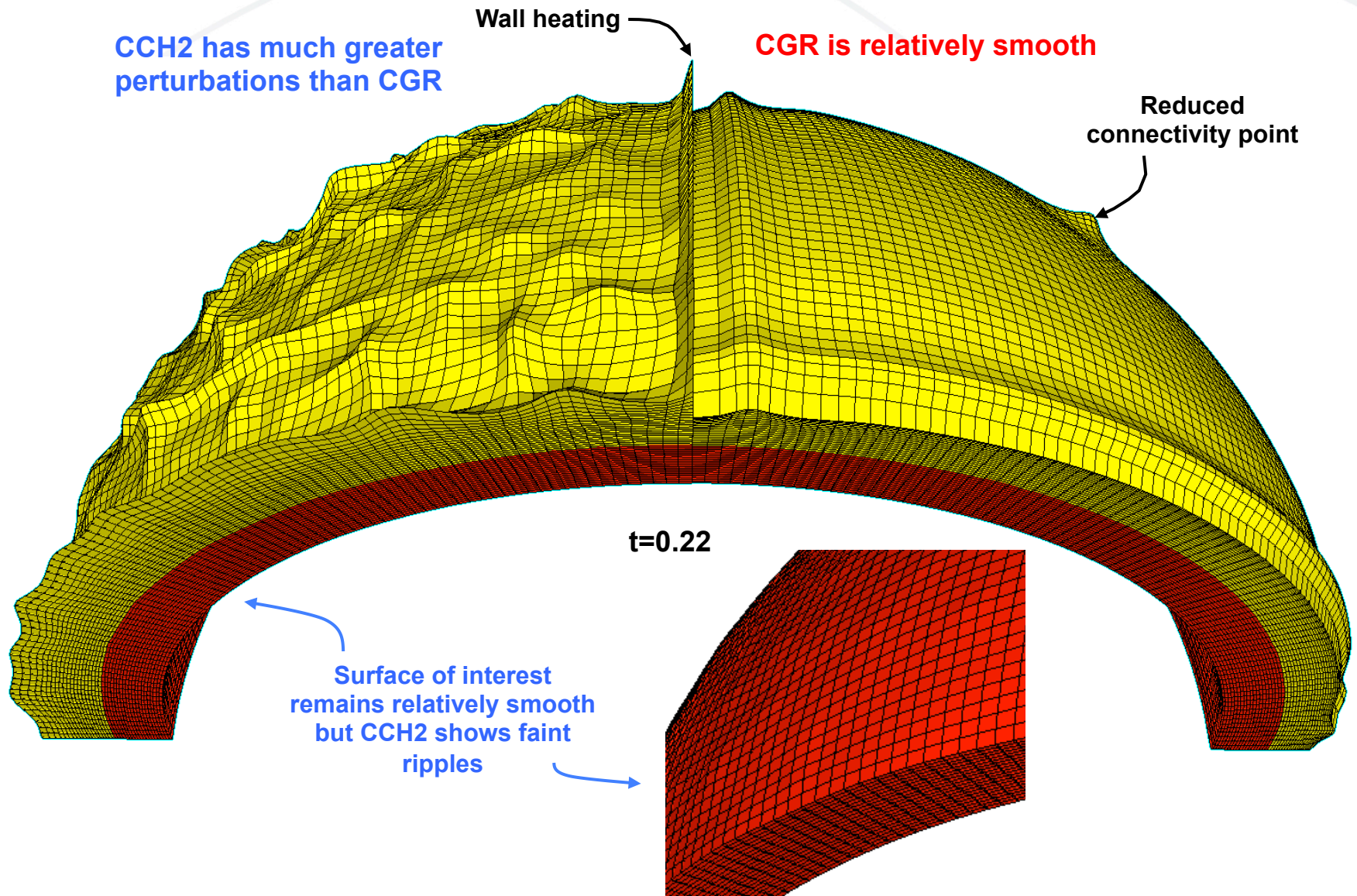
# 3D Kidder shell: Near perfect grids cannot be generated in 3D, resulting in much greater sensitivity to numerical error

As there exists no completely symmetrical tessellation of a sphere, numerical errors are larger in 3D

Pressure is applied at larger radius, so that the perturbations propagate inward



# The outer surface is hydrodynamically unstable and is especially sensitive to the numerical perturbations of CCH2





# SHOCK PROBLEMS

Sod

Noh

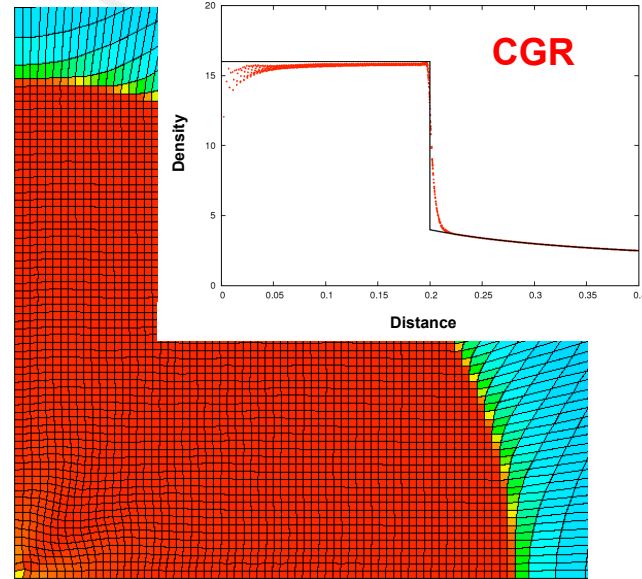
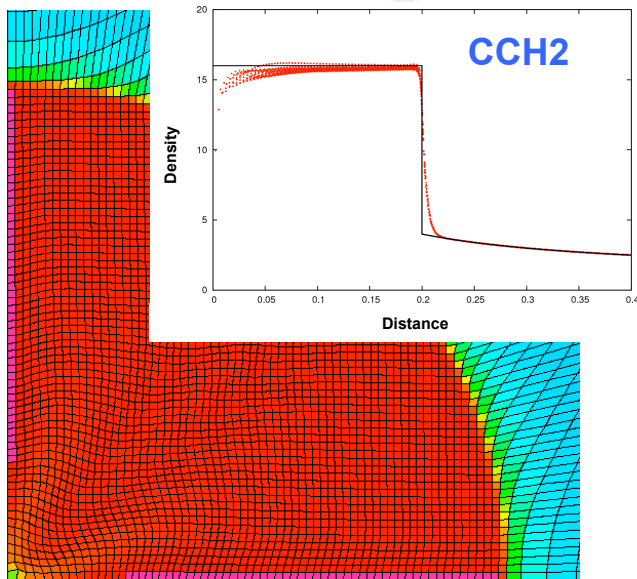
Sedov

Saltzman

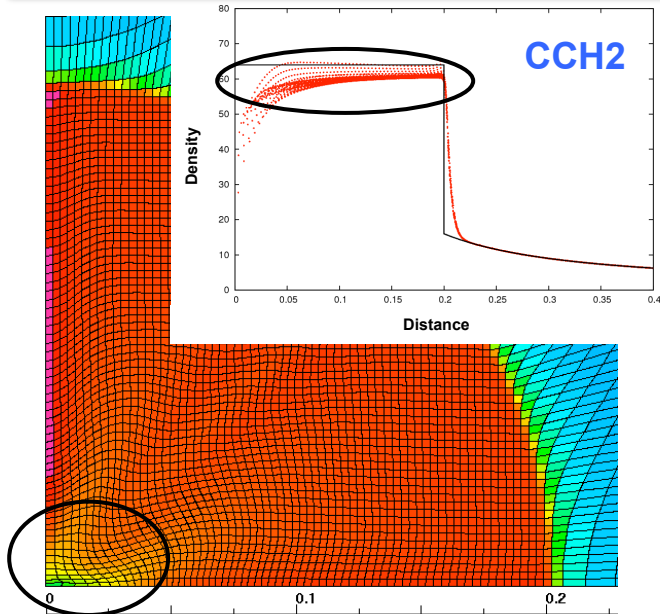
Elastic-plastic piston (solid)

Adiabatic release

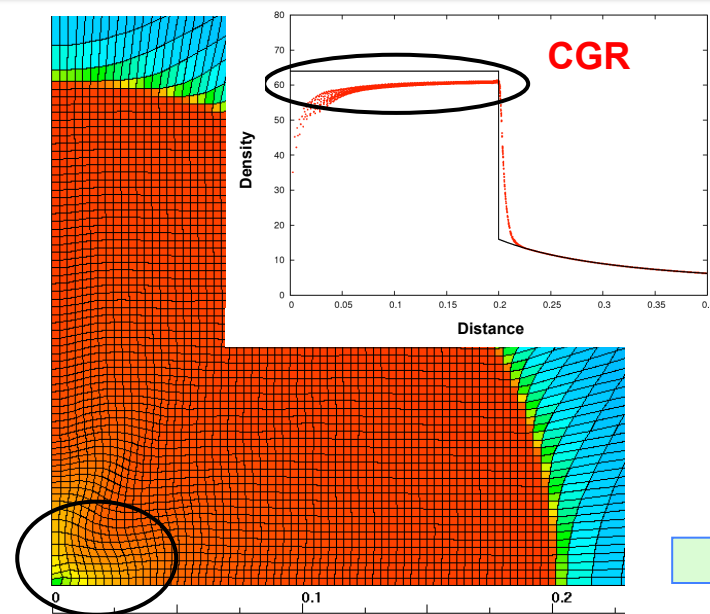
# 2D Noh on a box grid: results are comparable in XY, but CGR is clearly superior in RZ



XY



RZ



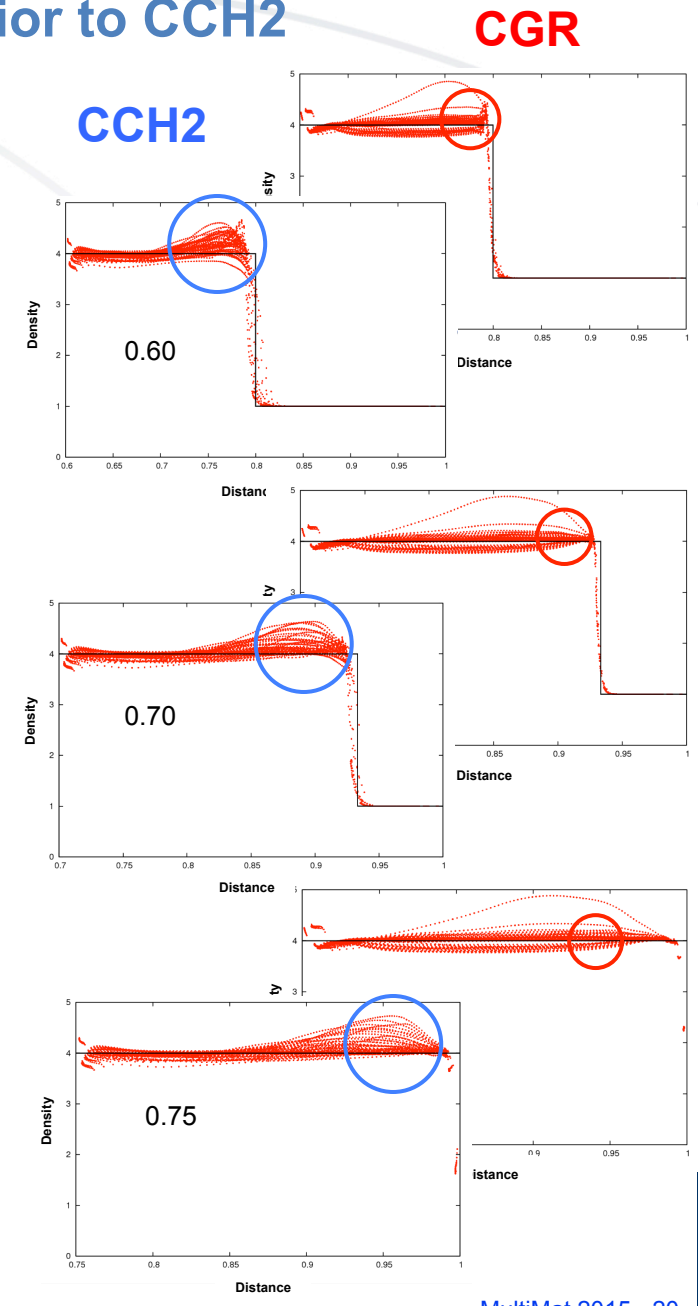
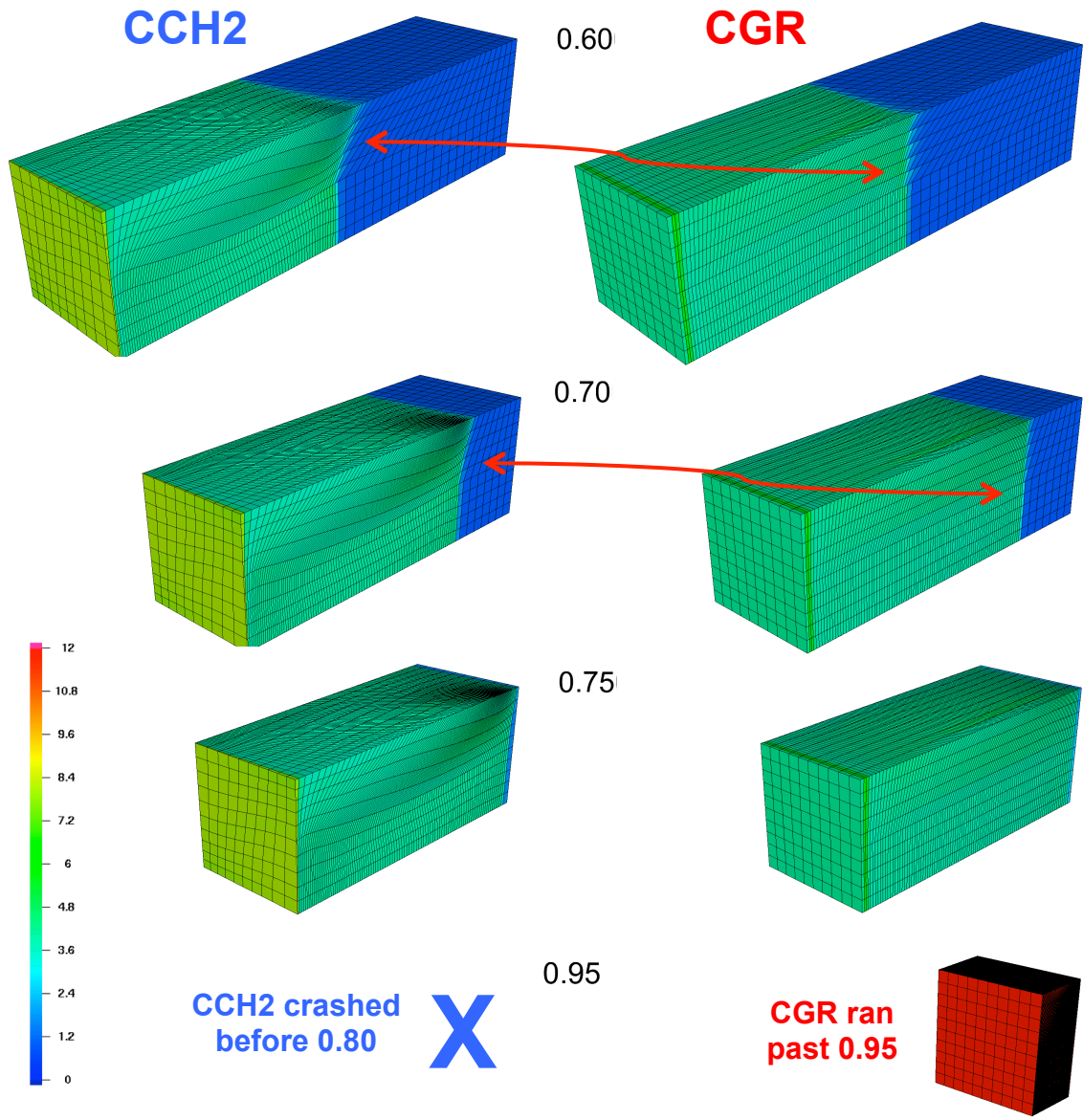
Scatter plots:  
one dot per cell

Exact solutions  
in black

Noh 1987

# The 3D skewed Saltzman mesh causes spurious vorticity: CGR results are far superior to CCH2

Caramana et al, 1999  
Maire et al, 2009  
Boscheri et al, 2014  
Burton et al, 2015



# ALE PROBLEMS

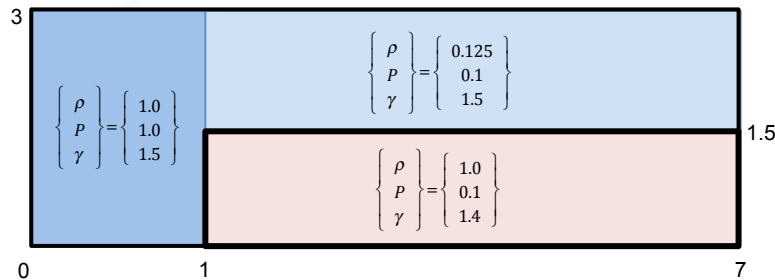
## Triple Point Helium Bubble

**xALE is an exact intersection  
2<sup>nd</sup> order remap scheme  
described at Multimat 2013**

**Swept is an unsplit 2<sup>nd</sup> order  
face advection scheme**

# Triple point problem: The combination CGR + xALE is significantly better than CCH2 and swept alternatives

The triple point problem simulates a shock hitting a material discontinuity, producing vortical flow

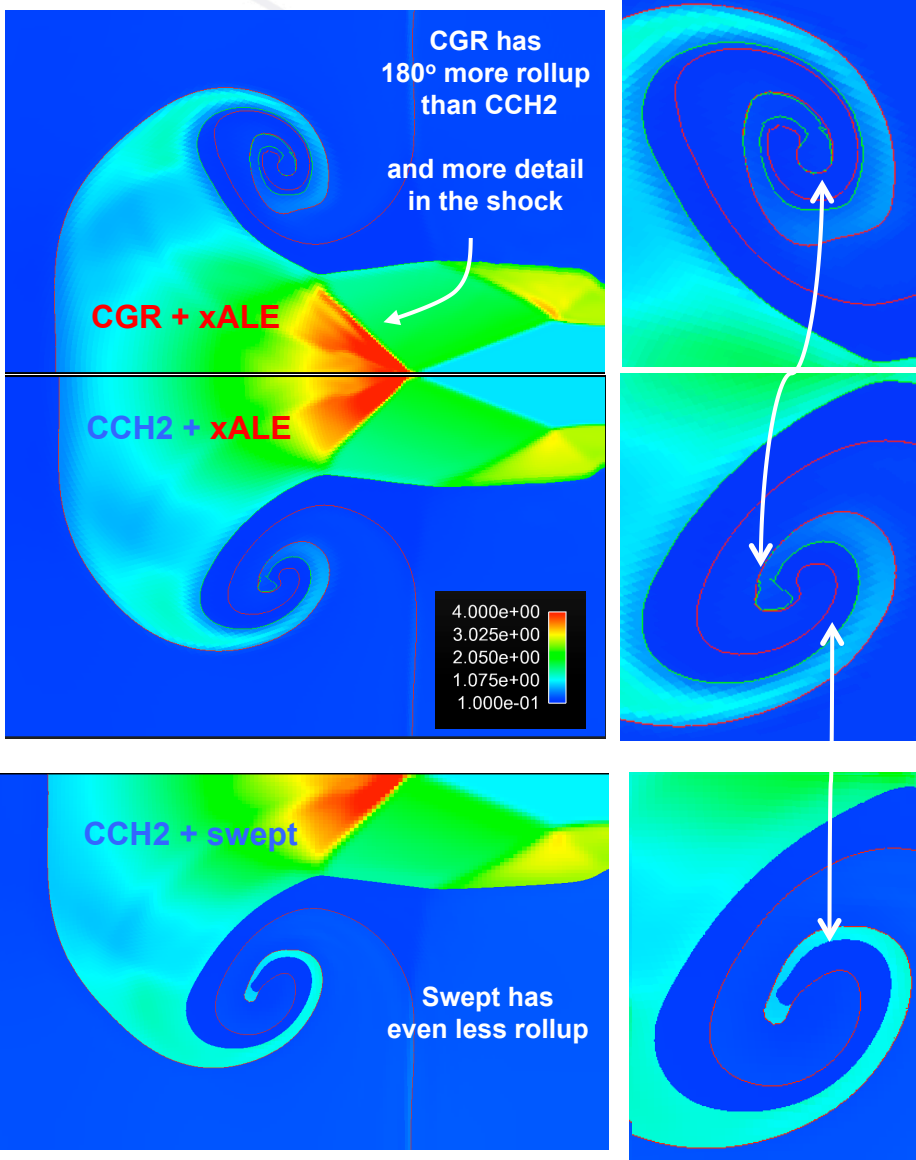


Although very early flow is self-similar, there is no converged solution at late times

The rollup at  $t=5.0$  should increase with resolution unless perturbed by numerical error, leading to Kelvin-Helmholtz instabilities

Mesh 200x100  
 $t=5.0$  density contours  
 Red & blue lines are material interfaces

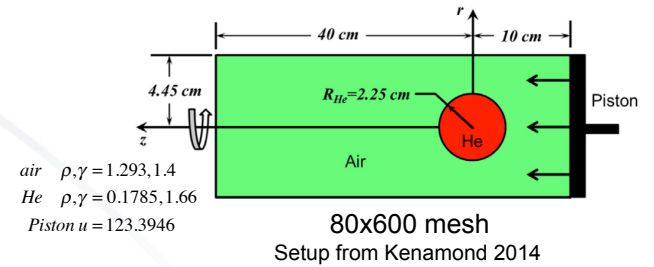
D'yadechko, 1965  
 Shashkov et al, 1991  
 Maire, 2009  
 Galera et al, 2010  
 Loubere et al, 2010  
 Burton et al, 2012



# Haas-Sturtevant helium bubble experiment: CGR has much less dissipation than CCH2 and a better match to data

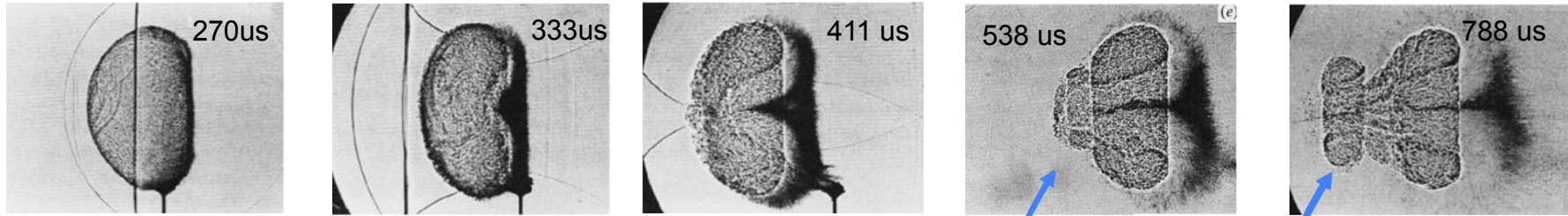
Haas & Sturtevant 1987  
 Quirk & Karni 1996  
 Galera et al 2010  
 Loubere et al 2011  
 Kenamond et al, 2014  
 Burton et al, 2015

**CGR matches Schlieren images  
 much better than CCH2**



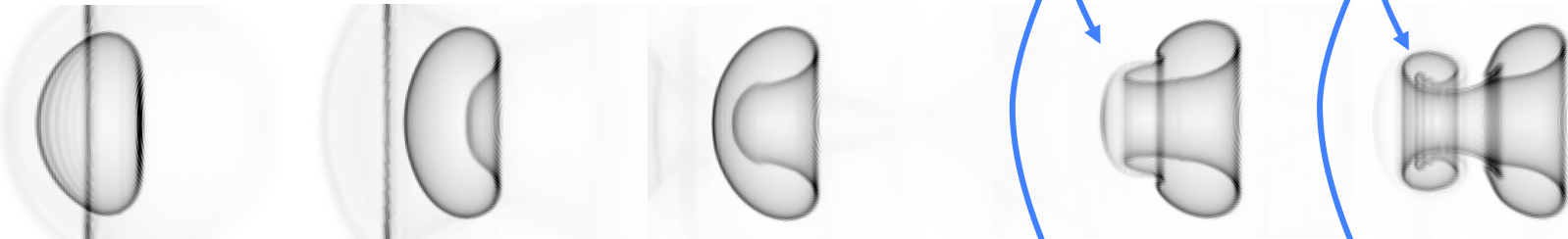
Schlieren images detect density gradient

Haas & Sturtevant JFM 1987, Fig 8

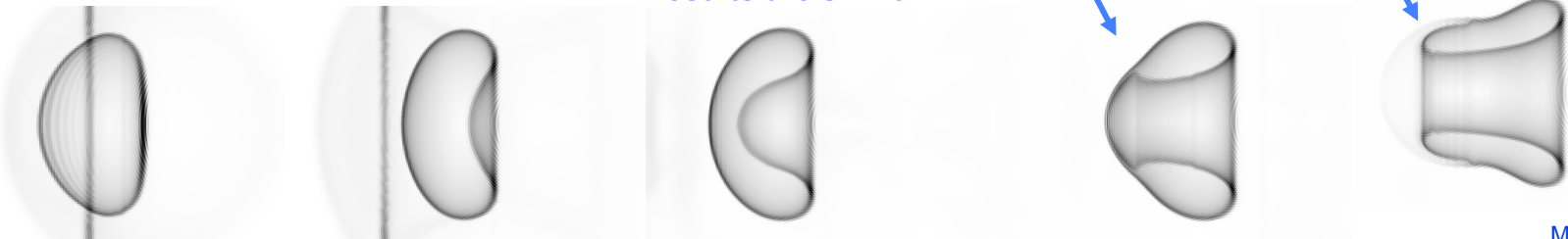


Synthetic Schlieren images

**CGR + xALE**



**CCH2+xALE and CCH2+swept  
 results are similar**



## Thoughts to take away

Our principal goal was to address excessive dissipation in CCH

- We have done so
- As demonstrated on a wide variety of test problems
- With results that are among the best we have seen

We introduced an extension to CCH called **Corner Gradient Reconstruction (CGR)**

- CGR differs from traditional CCH2 only in the reconstruction step
- Conceptually simple
- Does not require solving large systems of equations in each cell
- Multi-dimensional
- Applicable to solids and fluids
- Potentially beneficial to CCH formulations other than our own

CGR offers significant advantages over CCH2

- Improved directional accuracy
- Reduction in dissipation, especially for smooth flow problems
- Performs comparably or better for shocks
- Computational cost is comparable to CCH2

xALE exact intersection remap

- Following up on our MultiMat 2013 presentation, we have shown that **xALE** performs much better than **swept** face advection for vortical flows such as Taylor-Green



## 2D Verney (RZ) problem

Given an initial divergence free velocity field

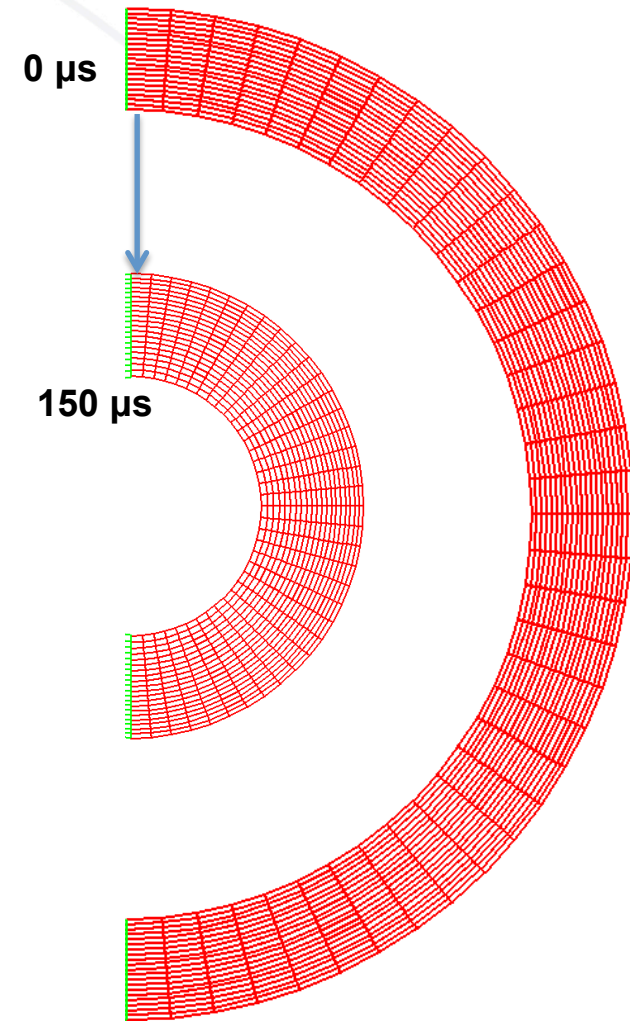
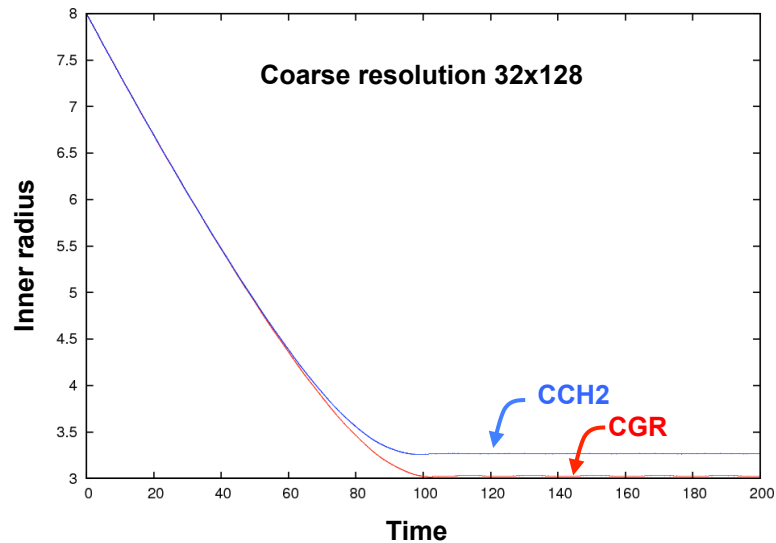
$$u(r) = u_0 \left( \frac{R_{outer}}{r} \right)^{\alpha-1}$$

An elastic-plastic shell is initially on the yield surface

It coasts inward until the kinetic energy is dissipated by plastic work

For an **INCOMPRESSIBLE** material, the analytic stopping radius is 3 cm

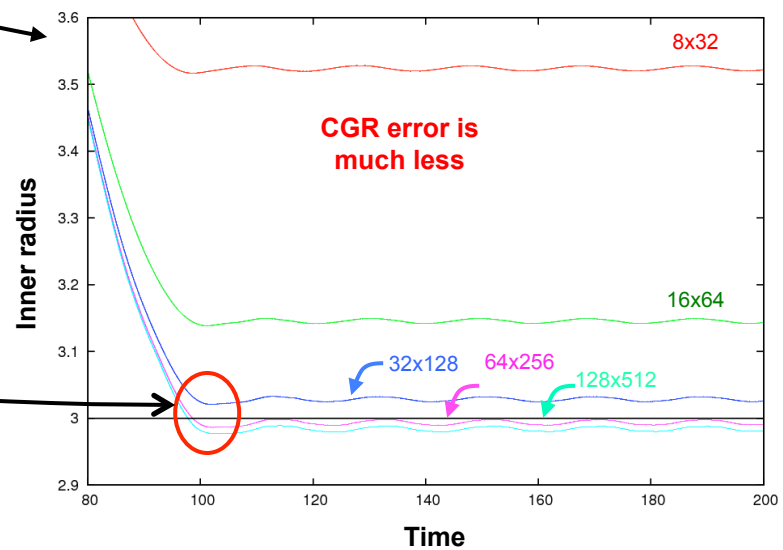
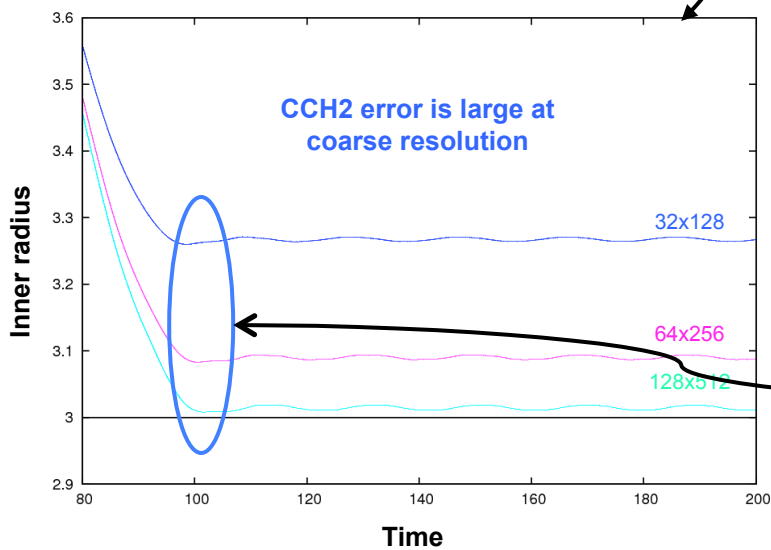
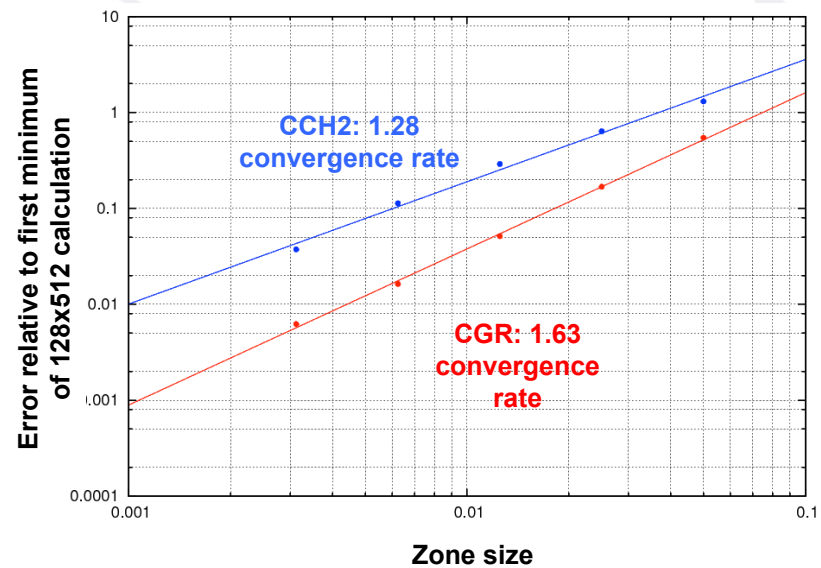
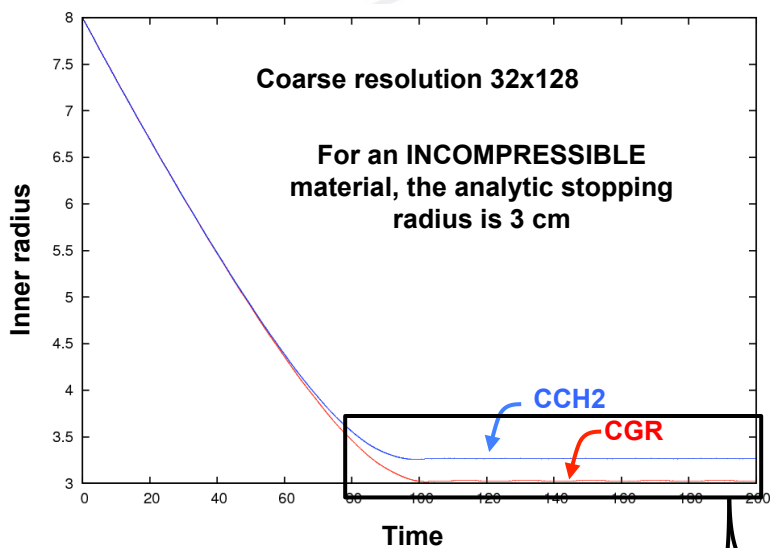
A **COMPRESSIBLE** material will have acoustic waves and overshoot



Verney 1968  
Howell & Ball 2002

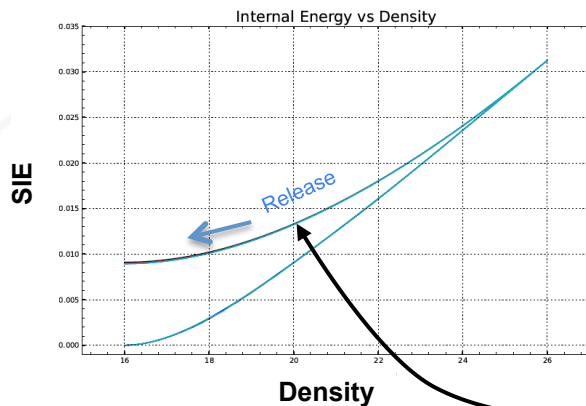
# 2D Verney

## CGR has much smaller error and higher convergence rate



# Adiabatic release problem tests the ability to track the adiabat following a shock compression

Base zoning  
90 cells  
 $h=10^{-2}$



$$p(\rho) = \left( \frac{\rho}{\rho_0} - 1 \right) \rho_0 c_0^2$$

$$u_p = \frac{1}{2} u_L$$

$$p_H = \rho_0 u_p (c_0 + u_p)$$

$$\rho_H = \rho_0 \left( 1 + \frac{u_p}{c_0} \right)$$

$$e_H = \frac{p_H (\rho_H - \rho_0)}{2 \rho_H \rho_0}$$

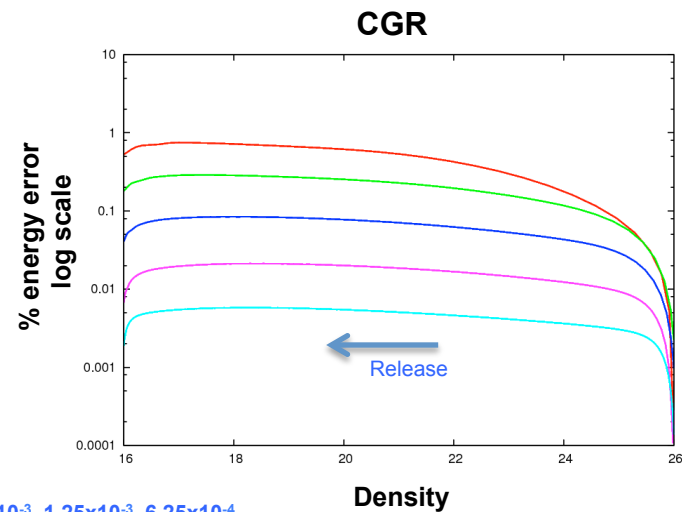
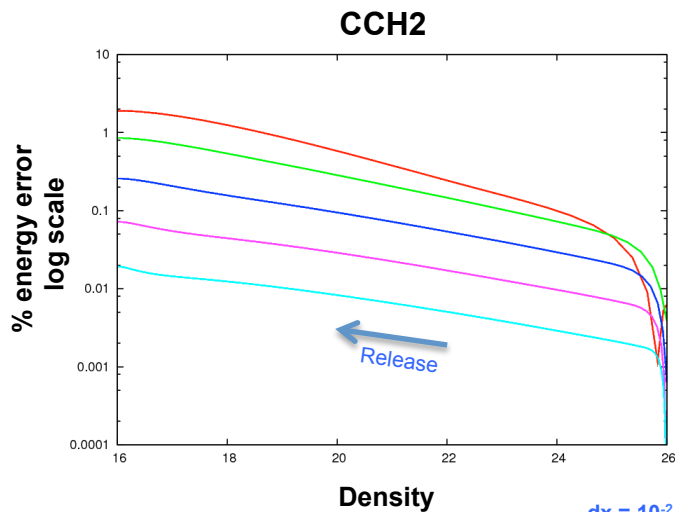
$$e_A(\rho) = e_H + c_0^2 \left[ \frac{\rho - \rho_H}{\rho_0} - \ln \left( \frac{\rho}{\rho_H} \right) \right]$$

Bazan & Rieben, LLNL-PRES-463883  
Owen et al, LLNL-PRES-557631  
Barlow 2011



Both are the best Lagrange results we have seen  
but CGR is superior to CCH2  
The error is less and more uniform over the release

Percent energy error at tracer location for various resolutions



$dx = 10^{-2}, 5 \times 10^{-3}, 2.5 \times 10^{-3}, 1.25 \times 10^{-3}, 6.25 \times 10^{-4}$

# The elastic-plastic piston problem tests the strength formulation at the elastic-plastic limit

The objective is to match speed and shape of the elastic precursor

Dissipation can mask the elastic precursor entirely

**The CGR results are sharper for both the elastic and plastic waves**

Piston velocity 10 cm/s  
 Aluminum properties:

- density  $\rho_0=2.79 \text{ g/cm}^3$
- shear modulus  $G=0.286 \text{ Mb}$
- yield stress  $Y_0=0.0026 \text{ Mb}$

Gruneisen EOS:

- $c_0=0.533$
- $s=1.34$
- $\Gamma=2.0$

